Lasing Characteristics of 2×4 Square Microcavity Laser Array

Wei Wang , Ke Yang, You-Ling Chen, Meng-Wei Sheng , Yue-De Yang, Jin-Long Xiao, and Yong-Zhen Huang

Institute of Semiconductors,

Chinese Academy of Sciences,

Beijing, China

Center of Materials Science and Optoelectronics Engineering,

University of Chinese Academy of Sciences

Beijing, China

yzhuang@semi.ac.cn

***Abstract*—A 2 x 4 semiconductor microcavity laser array of square microcavities with four waveguide ports is fabricated, forming two rows of microcavities, the upper row and the lower row. The wavelengths corresponding to the eight square microcavity units are identified through the spectra collected from different ports. The on-chip integration method lays the foundation for the application of multi-port light source and all-optical parallel digital computing.**

Keywords—semiconductor laser array, mode modulation, optical computing.

I. INTRODUCTION

In recent years, optical computing has drawn increasing research attention due to the advantages of high-speed parallel processing, low power consumption, high bandwidth and low crosstalk [1]. The development of traditional electronic computers is facing bottlenecks in power consumption, heat dissipation and speed of computing which is limited not only by the data transmission between memory and processing units, but also by the RC latency associated with integrated circuits. Efforts have been made in integrated photonic computing chips for optical computing and optical neural networks. All-optical signal processing and all-optical networks have the potential to replace conventional electronic integrated circuits [2, 3]. In all-optical network technology, all-optical logic gates provide the basic units for all-optical computing, switching and signal processing. Various all-optical logic gates with functions such as subtractors [4], differential equation solvers [5], storage elements [6, 7] and other computational techniques have been reported. Due to the merits of small size and low power consumption, microcavity lasers such as VCSELs and DFBs are well suited for the realization of on-chip all-optical logic gates [8, 9].

Here, a 2 x 4 semiconductor laser array of square microcavities with four waveguide ports is designed, containing two rows, the upper row and the lower row. The laser array is integrated on a two-dimensional mode surface. Integrated electrodes are designed at both rows to ensure that the same current is applied to each microcavity at the same row, simplifying the experimental operation. Simple fabrication processes, flexible integration methods, easy on-chip integration and multi-port light emission of the laser array facilitate the application in all-optical signal processing links. Larger scale on-chip integration can be achieved using high density integration techniques. In addition, the platform offers the possibility of wavelength multiplexing for parallel computing. This system thus sheds light on the next generation of all-optical computing systems. In terms of counter-surveillance, Moreover, this laser array is capable of producing multiple coherent light sources simultaneously that overlap with each other in space due to the multiple waveguides.

II. NUMERICLE SIMULATIONS

Two-dimensional finite element method (FEM) is used to simulate the microcavity laser array. The mode Q factors under different wavelengths for the single square microcavity with four waveguides of width d = 2 μm are shown in Fig. 1(a). Two sets of longitudinal modes ranging from 1525 nm to 1555 nm with fundamental modes located at 1531.6 nm (symmetric mode, SM) and 1549.1 nm (antisymmetric mode, ASM) can be found. The corresponding Q factors are 9435 and 4188, respectively. Mode field distributions of the fundamental ASM and SM are shown in Fig. 1(b). Fig. 1(c) shows the mode *Q* factors under different wavelengths for the laser array. There are 16 fundamental modes which can be found at the range of 1531.6 nm to 1531.7 nm with *Q* factors ranging from 3966 to 10012. These modes have different mode field distributions in different units. The mode field distribution |Hz| for the highest-*Q* mode is shown in Fig. 1(d).

III. DEVICE FABRICATION AND RESULTS

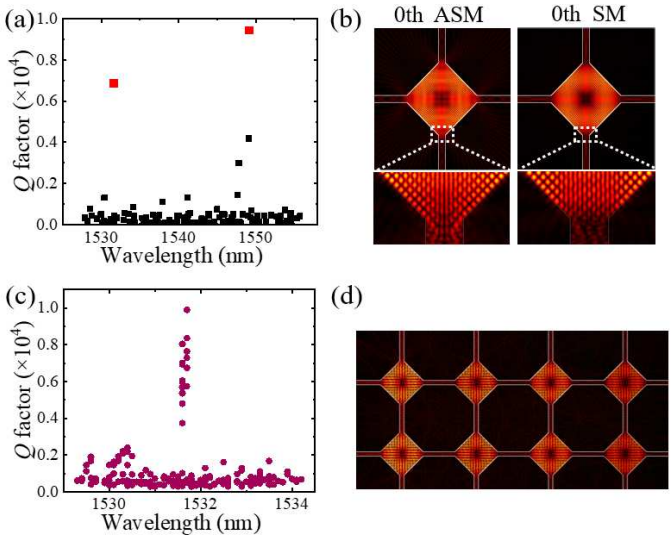

Fig.1. Mode Q factors versus wavelengths for the unit square microcavity (a) and the laser array (c). Mode field distribution |Hz| for the 0th SM and ASM of the unit square microcavity. Zoom in: enlarged view of the mode field distributions near one vertex. (b) and highest-Q mode in the laser array (d).

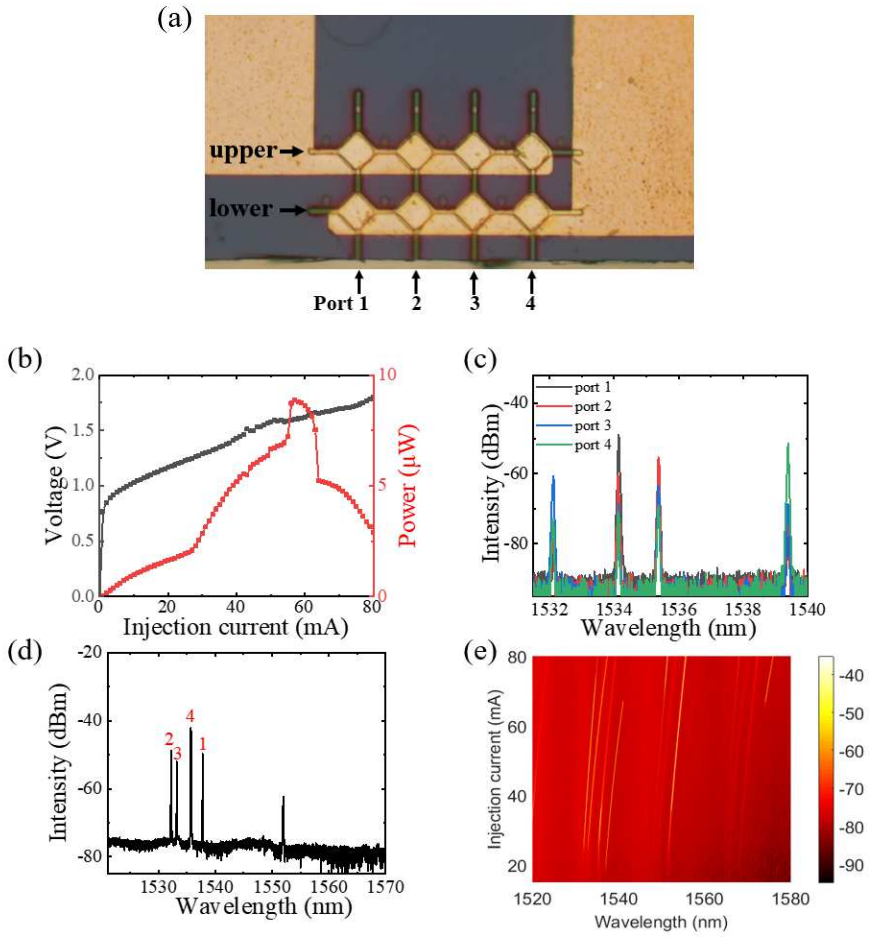

Fig.2. (a) Microscope image of the fabricated laser array. (b) Output power coupled to multi-mode fiber (MMF) and V-I curve at 293 K versus continuous injection current in the upper row from port 1. Emission spectra collected by MMF from the four ports independently at the injection current of 30 mA only in upper row(c), near port 2 at the injection current of 30 mA (d), and from 15 mA to 80 mA only in the lower row (e).

The array of square microcavities is fabricated using the AlGaInAs/InP epitaxial wafer with a photoluminance

wavelength of about 1517 nm. The active region with six compressively strained 6-nm-thick quantum wells and seven 9-nm-thick barrier layers is grown on the InP substrate by metal organic chemical vapor deposition. Contacting photolithography and ICP etching are employed to fabricate the array of square microcavities. The microcavity is laterally confined by a BCB layer for planarization. Afterward, a Ti/Pt/Au p-electrode is deposited by e-beam evaporation followed by lift-off process, and an Au/Ge/Ni metallization layer is deposited by magnetron sputtering as the n-electrode. The microscope image of the fabricated laser array is presented in Fig. 2(a). The output power coupled to multi-mode fiber (MMF) and the V-I curve at 293 K versus continuous injection current in upper row cavities from port 1 are illustrated in Fig. 2(b). The threshold current is 26 mA with the threshold current density of 1.28 kA/cm^2. The obviously lower threshold current may be attributed to better heat radiation induced by BCB lateral confinement. The maximum coupled powers is 8.9 μW at the continuous current of 57 mA.

Fig. 2(c) shows the emission spectra measured from ports 1, 2, 3 and 4 at the injection current of 30 mA applied to the upper row alone. Four peaks are located at 1532.11 nm, 1534 nm, 1535.37 nm and 1539.39 nm. It can be found that the first peak at 1532.11 nm has the highest intensity at port 3, as shown by the blue curve, indicating that this wavelength corresponds to the square microcavity in the upper row of port 3. The other three wavelengths correspond to the square microcavities in the upper row at ports 1, 2 and 4, respectively. The wavelength intervals of the four square microcavities at port 4, 1, 2 and 3 are 2.03, 1.23 and 4.02 nm, respectively. When an injection current of 30 mA is applied to the lower row alone, the spectrum is shown in Fig. 2(d). The MMF is located near port 2 to ensure that the intensities of the four wavelengths are almost consistent. The four peaks are located at 1532.22, 1533.22, 1535.70 and 1537.78 nm, corresponding to the square microcavities at ports 2, 3, 4 and 1 of the lower row, whose wavelength intervals are 1.00, 2.48 and 2.08 nm, respectively. Differences of the resonance wavelengths may be resulted from the differences in the dimensions of the square cavities in the fabrication process. From the differences in wavelengths, it can be inferred that the differences in the sizes of square microcavities are in the range of 9.7 – 71.2 nm. Fig. 2(e) shows the spectra near port 2 at the injection current range from 10 mA to 80 mA. The four wavelengths exit all the time. The redshift rates of the modes corresponding to the four square microcavities in the lower row at port 2, 3, 4 and 1 are 0.05, 0.7, 0.06 and 0.08 nm/mA.

IV. Conclusion

A 2 x 4 waveguide-connected square microcavity laser array has been fabricated, and the wavelengths of these eight microcavity units have been identified by the spectra at different ports. This laser array enables the in-plane integration of multiple light sources, and larger scale on-chip integration of laser arrays can be expected using high-density integration technique. The system can be used for all-optical signal processing links for applications such as complex logic calculations. Additionally, by fabricating independent electrodes between different cavities to control each cavity independently, various logic gates can be implemented. Graphic electrode can also be constructed to simulate 0th ASMs and SMs with different field distribution at the vertices independently, which can be used for parallel logic computing.

References

[1] R. S. Tucker and K. Hinton, "Energy Consumption and Energy Density in Optical and Electronic Signal Processing," IEEE Photon. J., vol. 3, no. 5, pp. 821-833, Oct 2011.

[2] D. Van Thourhout, T. Spuesens, S. K. Selvaraja, L. Liu, G. Roelkens, R. Kumar, et al., "Nanophotonic Devices for Optical Interconnect," IEEE J Quantum Electron, vol. 16, no. 5, pp. 1363-1375, Sep-Oct 2010.

[3] R. Nagarajan, M. Kato, J. Pleumeekers, P. Evans, S. Hurtt, A. Dentai, et al., "Large-scale photonic integrated circuits," International Conference on Indium Phosphide and Related Materials, Matsue, JAPAN, pp. 32-34, May 2007.

[4] R. Nagarajan, M. Kato, J. Pleumeekers, P. Evans, S. Hurtt, A. Dentai, et al., "Large-scale photonic integrated circuits," International Conference on Indium Phosphide and Related Materials, Matsue, JAPAN, pp. 32-34, May 2007.

[5] K. S. Chen, J. Hou, Z. Y. Huang, T. Cao, J. H. Zhang, Y. Yu, et al., "All-optical 1st-and 2nd-order differential equation solvers with large tuning ranges using Fabry-Perot semiconductor optical amplifiers," Opt. Express, vol. 23, no. 3, pp. 3784-3794, Feb 2015.

[6] M. T. Hill, H. J. S. Dorren, T. de Vries, X. J. M. Leijtens, J. H. den Besten, B. Smalbrugge, et al.,"An ultra-small, low-power, all-optical flip-flop memory on a silicon chip," Nat. Photonics, vol. 4, no. 3, pp. 182-187, Mar 2010.

[7] M. T. Hill, H. J. S. Dorren, T. de Vries, X. J. M. Leijtens, J. H. den Besten, B. Smalbrugge, et al., "A fast low-power optical memory based on coupled micro-ring lasers," Nature, vol. 432, no. 7014, pp. 206-209, Nov 2004.

[8] S. Y. Xiang, Z. X. Ren, Z. W. Song, Y. H. Zhang, X. X. Guo, G. Q. Han, et al., "Computing Primitive of Fully VCSEL-Based All-Optical Spiking Neural Network for Supervised Learning and Pattern Classification," IEEE Trans Neural Netw Learn Syst, vol. 32, no. 6, pp. 2494-2505, Jun 2021.

[9] S. Xiang, Y. Han, Z. Song, X. Guo, Y. Zhang, Z. Ren, et al., "A review: Photonics devices, architectures, and algorithms for optical neural computing," J. Semicond., vol. 42, no. 2, 2021.